Farmland human-shape obstacles identification based on Viola-Jones Algorithm

Linlin Wang[1,2], Wenwei Xiao[2,3], Yuan Qi[2,3], Qichao Gao[2,3], Lin Li[3], Kangting Yan[2,3], Yali Zhang[2,3*], Yubin Lan[1,2*]

(1. *College of Electronic Engineering, South China Agricultural University, Guangzhou* 510642, *China*;
2. *National Center for International Collaboration Research on Precision Agricultural Aviation Pesticides Spraying Technology, Guangzhou 510642, China*;
3. *College of Engineering, South China Agricultural University, Guangzhou* 510642, *China*)

Abstract: When agricultural unmanned aerial vehicle (UAV) is spraying in the field or hovering on the ridge, there is a possibility that obstacles without moving characteristics represented by humans may collide with agricultural UAV. In order to quickly identify and detect human-shape obstacles, realize the safe operation of agricultural UAV, this paper proposes a new method based on Viola-Jones Algorithm according to the head-shoulder ratio characteristics of Chinese adults and the basic spraying parameters of agricultural UAV. The cascade object detector is used to detect people's upper bodies area of all humanoid obstacles in the view field of the agricultural UAV's flight direction, and the extracted upper body image is binarized to obtain the relevant projection histogram and calculate the width ratio and distance ratio of head-shoulder, then judge whether it is a human-shape obstacle, and combine the depth and position information to avoid the danger of collision. The test results show that the method is feasible and effective in recognizing human-shape obstacles on the front or back in the farmland within the sight distance of 6 meters.

Keywords: agricultural UAV, binocular vision, picture processing, human-shape obstacles, MATLAB
DOI: 10.33440/j.ijpaa.20200303.99

Citation: Wang L L, Xiao W W, Qi Y, Gao Q C,Li L, Yan K T, Zhang Y L, Lan Y B. Farmland human-shape obstacles identification based on Viola-Jones Algorithm. Int J Precis Agric Aviat, 2020; 3(3): 35–40.

1 Introduction

In the Joint Circular of the General Offices of MOA, the Ministry of Finance (MOF) and the Civil Aviation Administration of China on Launching Pilot Programs of Farm Machinery Purchase Subsidy for Standard Operation of Plant Protection Drone released in September 2017, it was for the first time clearly specified that pilot drones should be equipped with an obstacle avoidance system so that the flight operation can identify, monitor and trace the surrounding environment[1]. And in January 2018, the Interim Regulations on flight management of UAVs (Draft for comments) stressed that ensuring flight safety and important target safety should be considered as the focus of legislative work[2]. The Interim Regulations on flight management of UAVs (Draft for approval) submitted in July 2019 pointed out the urgent need to formulate top-level regulations to regulate operations, better maintain national, public and flight safety, and promote the rapid and healthy development of UAV industry and related fields. Therefore, the realization of intelligent perception of farmland obstacles and real-time obstacle avoidance is one of the development trends of intelligent agricultural drones, which can improve the safety of production[3,4]. Obstacle avoidance systems based on visual sensors, for example, binocular vision sensors can detect obstacles at different distances by changing the baseline. It is more intuitive and clearer in identifying obstacle types, depth information, and recording flight data[1].

In the image feature extraction of target detection, common methods include HOG (Histogram of Oriented Gradient) features, LBP (Local Binary Pattern) features, Haar-like features, etc. HOG features constitute the feature by calculating and counting the gradient direction histogram of the local area of the image[5]. The HOG+SVM classifier has been widely used in image recognition. It can better describe the shape, weaken the influence of illumination, and has a good effect in pedestrian recognition. LBP features is an operator used to describe local texture features of an image. With low dimension and fast computing speed, LBP texture features have significant advantages such as rotation invariability and gray invariability[6]. However, when the illumination changes are not uniform, the size relation between each pixel is destroyed and the corresponding LBP operator also changes. Haar-like features is a very classic feature extraction algorithm. Haar feature value reflects the change of image gray level and can better describe the change of light and shade[7]. It is sensitive to some simple graphic structure, such as edge and line segment, and suitable for describing the structure with specific strike (horizontal, vertical and diagonal)[8]. Haar and LBP

Received date: 2020-08-25 **Accepted date:** 2020-09-17
Biography: Linlin Wang, PhD candidate, research interests: farmland obstacle avoidance, Email: 576150990@qq.com; **Wenwei Xiao**, master student, research interests: detection of floret opening in rice, Email: 910101568@qq.com; **Yuan Qi**, master student, research interests: UAV remote sensing image processing, Email：yuanqi@stu.scau.edu.cn; **Qichao Gao**, master student, research interests: pesticide spraying on sugared oranges, Email: 18864832285@163.com; **Lin Li**, undergraduate, research interests: binocular vision, Email: 1084708453@qq.com; **Kangting Yan**, master student, research interests: pesticide residue detection based on fluorescence spectroscopy, Email: keepingykt@163.com.
*** Corresponding author: Yali Zhang**, PhD, Associate Professor, research interests: precision agricultural sensor for UAV, Mailing Address: South China Agricultural University, Wushan Road, Tianhe District, Guangzhou City, Guangdong, 510642, China. Email: ylzhang@scau.edu.cn; **Yubin Lan,** PhD, Professor, research interests: precision agricultural aviation application. Mailing Address: South China Agricultural University, Wushan Road, Tianhe District, Guangzhou City, Guangdong, 510642, China. Email: ylan@scau.edu.cn.

features are often used to detect faces because they work well for representing fine-scale textures. The HOG features are often used to detect objects such as peopleand cars. They are useful for capturing the overall shape of an object[9,10]. Based on AdaBoost algorithm, Viola and Jones construct viola-Jones detector by using Haar-like feature and integral graph method for face detection[11].

This paper proposes a new method based on Viola-Jones algorithm according to the head-shoulder ratio characteristics of Chinese adults and the basic spraying parameters of agricultural UAV. The cascade object detector is used to obtain the upper body area of all humanoid obstacles in the view field of the agricultural UAV's flight direction, and binarize the extracted upper body image to obtain the relevant projection histogram, then calculate the ratio of the maximum head width W_H (as shown in Figure 1) to the maximum shoulder width W_S (marked as the width ratio of head-shoulder, R_{HS1}),and the ratio of the maximum head width W_H to vertical distance D from top of head to maximum shoulder width(marked as the distance ratio of head-shoulder, R_{HS2}), then judge whether it is a human-shape obstacle and whether there is collision risk according to the depth and position information, so as to realize the rapid identification and detection of human-shape obstacles and ensure the safe operation of agricultural UAVs.

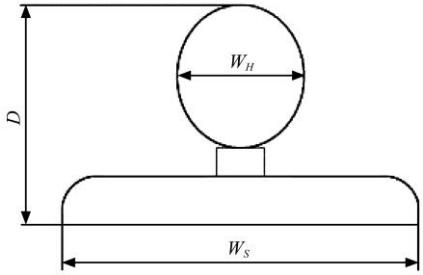

Figure 1 Upper body model

2 Theory and testing

In the actual spraying environment, the flying height of the agricultural UAV is 1-3 m from the crop canopy, and the flying speed is about 3-6 m/s[12,13]. Obstacles affecting its flight include various man-made facilities, various organisms with irregular action in the flying range, as well as instruments in agricultural production. According to the characteristics of obstacles, all kinds of farmland obstacles that may appear in the working environment can be classified into four categories[1], as shown in Table 1.

Table 1 Size-based farmland obstacles classification

Type	Example
Micro obstacles	wire, inclined cable, branch, protruding plant, power grid or communication line, wooden pole or pergola placed in the field, test pole, nylon net, metal net, etc.
Small and medium obstacles	scattered tree, telegraph pole, hayrick, wind turbine, etc.
Large obstacles	shelter forest, high-pressure tower, house, meteorological tower, etc.
Non-fixed or visually-distorting obstacles	bird and beast, human being, high-speed moving non-living objects, blurring-texture or specular- reflecting objects, for instance, pond, plastic film in greenhouse, PC sun sheet, etc.

At present, agricultural UAV has been able to identify large and medium-sized obstacles. Other non-living objects cannot move independently, so if the obstacle avoidance system of agricultural UAV is sensitive and mature enough, accidents such as fuselage damage or crop loss can be avoided. Among the above obstacles, human being and animals are obstacles that can move actively. However, the scope of human movement is more complicated, and it also involves the management regulations of legal operation and safety of pesticide spraying, so the safety of human life is the most concerned issue of our obstacle avoidance research. When the agricultural UAV sprays in the field or hovers on the ridge to take off or land, the primate obstacles with no regular motion characteristics represented by humans, who are in the operation range of agricultural UAV, if their attention is concentrated, they can withdraw from the agricultural UAV's work area actively because of their sensory organs. However, when people's attention is distracted, senses are degraded, or the human body is blocked by vegetation in the operating area, there is a possibility that the passive obstacle avoidance system of agricultural drone cannot detect human-shape obstacles, or that a person riding fast-moving vehicles on ridges may hit agricultural drones in the non-applied state, either of which will cause a serious safety accident.

2.1 Characteristic analysis of human-shape obstacles

Compared with other obstacles, human-shape obstacles can be distinguished quickly from micro obstacles such as electric wires and large obstacles such as houses according to their size. Among obstacles with insignificant differences in volume, factors such as the height or size cannot be easily distinguished, but the outline and structure of human-shape obstacles are clearly different from other small and medium-sized obstacles. For example, the curvature changes of obstacles such as electric poles and haystacks are obviously different from those of human body, and the structural proportions of height, area and other parts of agricultural machinery such as turbines also have nothing in common with those of human body.

At the same time, due to differences between individuals, human-shape obstacles have greater uncertainty in some characteristics, such as height, weight, and clothing. In the farmland operating environment, the part below the head of people may be blocked by the external environment or Interfering with clothing. If such factors are identified as the characteristics of human-shape obstacles, it is not general and cannot effectively identify all human-shape obstacles. Although the contour of human body can accurately represent the features of most human-shape obstacles, if the entire contour is chosen as the recognition feature, because the contour shape of most areas changes during the human body is moving[14], it is hard to identify the contour features by setting simple and fast standards.

Based on the upper body model (as shown in Figure 1), this paper selects local scale features to realize the recognition of human-shape obstacles, and selects two indexes that the width ratio of head-shoulder R_{HS1} and the distance ratio of head-shoulder R_{HS2} to realize the recognition of human-shape obstacles. Process the picture to obtain the target data, and judge whether each value is within a certain error range. Because individual differences have little effect on the proportion of human body structure, and the head and shoulders have movement stability[8], the selection of human-shape obstacle features combines the height and width of human head and shoulders, which can basically distinguish from other small and medium-sized obstacles.

According to the Chinese Adult Human Body Size Standard GB10000-1988[15], the R_{HS1} of adult men aged 18-60 is between 0.30-0.47, and the R_{HS2} is between 0.54-0.71, and that of adult women aged 18-55 R_{HS1} is between 0.29-0.44, and the R_{HS2} is between 0.56-0.72. After combining the above data, the R_{HS1} of the human-shape obstacle should be between 0.29-0.47 and the

R_{HS2} is between 0.54-0.72.

2.2 Method

This experiment uses the global exposure binocular camera Iris550 (as shown in Figure 2) of Supernode Innovative Technology Co., Ltd., with a binocular baseline of 55 mm, which is suitable for short-distance obstacle avoidance. When the binocular camera performs stereo matching, the target feature is unstable due to external factors, which reduces the detection accuracy of the target obstacle. In order to avoid the impact of information loss on the recognition result, the left lens is selected by default to extract and detect human-shape targets.

Figure 2 Supernode binocular camera Iris550

Due to the wide range of human activities and the great uncertainty of the activity route, people who are far away cannot be determined whether they will block the operation. Only the obstacles within a certain distance will hinder the normal spraying of agricultural UAV. For a range within 2 meters, as the operational flight speed of agricultural UAV is 3-6 m/s and has motion inertia, humans also have a certain speed when moving, recognition within this range is of no help to prevent collision accidents. At the same time, the fastest response time of humans has individual differences. When the agricultural UAV flies at a speed of 6 m/s, assuming that the reaction time of a person in stationary state is 1 second, the safety distance is at least 6 meters to avoid accidents. Combined with the safe distance range of human, the early warning range of agricultural UAV is artificially set beyond 6 meters, and the execution range of obstacle avoidance action is within 6 meters. Therefore, 2-6 meters are selected as the testing range for detection in this paper. In order to ensure there are obvious changes in the obstacle pictures at different distances, this paper uses 1 meter as the interval for testing.

According to the Report on Nutrition and Chronic Disease Status of Chinese Residents (2015)[16], the average height of adult men and women aged 18 and older is 167.1 cm and 155.8 cm respectively. Agricultural drones fly at a height of 1-3 m from the crop canopy during normal operation. When they are on the same horizontal plane and the vertical height is greater than 2 m, the probability of the aircraft directly hitting a person is small, which is regarded as a relatively safe critical height. However, when the UAV's flying height is less than 2 meters, it is easy to directly collide with people. Therefore, in the experiment, the testing height of Iris550 is set to 1 meter.

2.3 Algorithm

In this algorithm, firstly use the left lens to collect the front and back images of human-shape obstacles at different intervals of 2-6 m. Then, according to the collecting images, use the cascade object detector[17-19] combined with the elliptical skin color model to distinguish human-shape upper bodies from the environment, which parameters are selected based on prior experience. At the same time, select the largest connected area as the target area, complete the extraction of human-shape obstacle's upper body, binarize the extracted image, and obtain the horizontal projection histogram. According to the acquired horizontal projection histogram, the contour structure information of the upper body and the relevant data of special points are obtained. R_{HS1} and R_{HS2} are calculated to determine whether they conform to the relevant structural data of human body. When it is identified as a person, the depth information is combined to make the next obstacle avoidance judgment. The specific process is shown in Figure 3.

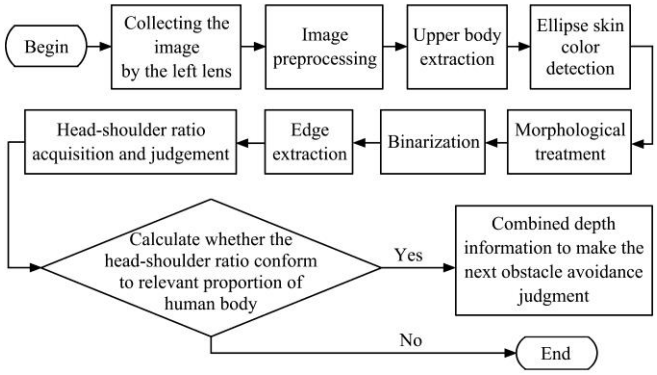

Figure 3 Head-shoulder ratio recognition flowchart

The Otsu algorithm[20] is used for image binarization, which is considered as the best algorithm for threshold selection in image segmentation. It is simple to calculate and is not affected by image brightness and contrast. It divides the image into two parts, the background and the foreground, according to the gray characteristics of the image. When the optimal threshold is taken, the variance between the two should be the largest.

Its mathematical formulation is as follows, divide the pixel value of the object picture into G gray levels [1, 2, …, G], use n_i to represent the number of pixels of level i, then it is easy to get the total number N of pixels as,

$$N = n_1 + n_2 + ...n_G \tag{1}$$

The gray-lever histogram is normalized and regarded as a probability distribution:

$$P_i = \frac{n_i}{N},\ P_i \geq 0,\ \sum_{i=1}^{G} P_i = 1 \tag{2}$$

Dichotomize the pixels into two classes C_b and C_o (background and objects) by a threshold at level k, C_b denotes pixels with levels [1, 2, …, k] and C_o denotes pixels with levels [k+1, k+2, … G]. Then the mean values of these two classes of pixels are m_b and m_o, and the global mean value of the image is m. At the same time, the probability of class occurrence is p_b and p_o respectively, those are given by

$$P_b = \sum_{i=1}^{k} P_i,\quad m_b = \frac{1}{p_b} * \sum_{i=1}^{k} iP_i \tag{3}$$

$$p_o = \sum_{i=k+1}^{G} P_i = 1 - p_b,\quad m_o = \frac{1}{p_o} * \sum_{i=k+1}^{G} iP_i \tag{4}$$

$$m_b * p_b + m_o * p_o = m \tag{5}$$

The expression of between-class variance σ^2 is

$$\sigma^2 = p_b(m_b - m)^2 + p_o(m_o - m)^2 \tag{6}$$

(due to (3-5)) and

$$\sigma^2 = \sum_{i=1}^{k} P_i \sum_{i=k+1}^{G} P_i \left(\frac{1}{p_b} * \sum_{i=1}^{k} iP_i - \frac{1}{p_o} * \sum_{i=k+1}^{G} iP_i\right)^2 \tag{7}$$

Traverse 0~255 gray levels, the gray level k that maximizes σ^2 is the optimal threshold k^*, and the probability of misclassification is minimum. The k^* is used for image binarization segmentation, then extract edge of the upper body in

binary image. In horizontal projection histogram, the -axis represents the number of rows, and the Y-axis represents the number of white pixels in the row. As shown in Figure 4, the upper limit of the X-axis in the histogram can be determined as the overhead point $A(x_A, y_A)$, and the maximum value near the point is determined as the head width W_H, which is recorded as $B(x_B, y_B)$, namely $W_H = y_B$. Since the maximum shoulder width W_S is 2.12-3.45 times of the maximum width of the head W_H, find the point $C(x_C, y_C)$ with the maximum curvature in $2.12W_H \le y \le 3.45W_H$, and the ordinate of point C can be regarded as the maximum shoulder width W_S, that is $W_S = y_C$. The distance from point A to point C can be regarded as the vertical distance D from top of head to maximum shoulder width, then $D = x_C - x_A$. According to the proportional relation shown in Eq. (8),

$$R_{HS1} = \frac{W_H}{W_S},\ R_{HS2} = \frac{2W_H}{D} \tag{8}$$

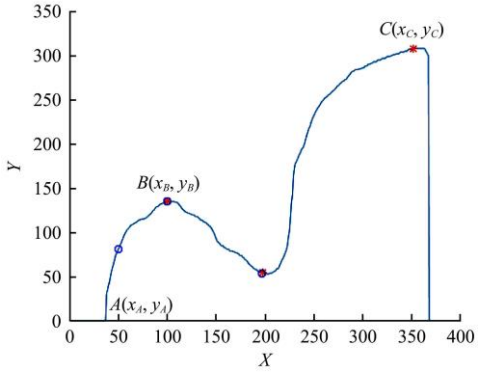

Figure 4 Horizontal projection histogram of human-shape obstacles

The cascade object detector uses the Viola-Jones algorithm[11] to detect upper body, which can detect object categories whose aspect ratio does not vary significantly. The vision.CascadeObjectDetector System object detects objects in images by sliding a window over the image. The detector then uses a cascade classifier to decide whether the window contains the object of interest. The size of the window varies to detect objects at different scales, but its aspect ratio remains fixed. The detector is very sensitive to out-of-plane rotation, because the aspect ratio changes for most 3-D objects. Thus, we only train a detector for front and back orientation of the human-shape obstacle, the training image size is [18 22]. The upper body is detected, which is defined as the head and shoulder areas. This model uses the haar function to encode detailed information about the head and shoulder areas. Because it uses more functions around the head, this model is more reliable for posture changes (such as head rotation).

2.4 Test environment

In order to verify the feasibility of the algorithm identification, Iris550 was used for indoor and outdoor experiments in different scenes, such as the Heyuan Laboratory of South China Agricultural University, the bushes and the cement road in the sugar orange orchard in Sihui, Guangdong. In the test, a man with height of 178 cm and weight of 90 kg and a woman with height of 165 cm and weight of 51 kg were respectively taken as human-shape obstacles. The height of Iris550 was set as 1m to simulate the hovering height of the agricultural UAV. Images of human-shape obstacles were collected at intervals of 1 m within the test distance of 2-6 m, as shown in Figure 5 and Figure 6.

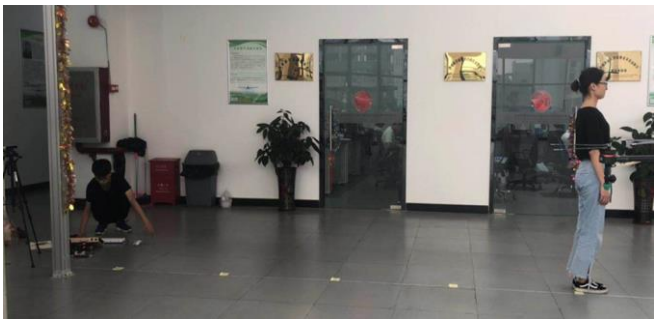

Figure 5 Indoor experiment in Heyuan

Figure 6 Outdoor experiment in sugar orange orchard of Sihui

The human-shape obstacle recognition algorithm was compiled in the MATLAB R2019a compiler. The error rate of R_{HS1} and R_{HS2} was set as ±2%, and the following three groups of tests were selected for explanation, laboratory environment, farmland environment and farmland cement road. According to the characteristics of a human-shape obstacle selected above, when $R_{HS1} \in [0.29, 0.47]$ and $R_{HS2} \in [0.54, 0.72]$, it can be identified as a human-shape obstacle.

3 Analysis and discussion

In the indoor test of Heyuan laboratory (as shown in Figure 7), taking the back image at a distance of 5m as an example, the algorithm will mark all the suspected human-shape obstacles in the scene, including human-shaped obstacles, potted plants, door frames and Paper cutting, etc., binarize all suspected human-shape obstacles, calculate R_{HS1} and R_{HS2} according to the horizontal projection histogram, and determine whether there are human-shape obstacles in the picture. In this test, the human head- shoulder ratio feature can be used effectively to distinguish all human-shape obstacles. However, the intensity and complexity of the indoor environment cannot fully simulate the farmland environment.

In view of the accidental collision of pedestrians walking on the ridges, each dataset of the male tester was randomly identified and judged. The test scene is shown in Figure 8, Table 2 shows the identification results and depth information of male tester on the cement road in the farmland environment.

Table 2 Test results of human-shape obstacle on cement road in farmland

Standard distance/m	R_{HS1}	R_{HS2}	Depth/m	Test angle	Judgement
1.999	0.42336	0.57727	1.989	Front	T
2.999	0.37500	0.54545	3.117	Back	T
4.001	0.37129	0.54348	4.184	Back	T
4.999	0.45770	0.55758	5.213	Front	T
6.001	0.48538	066529	6.269	Back	F

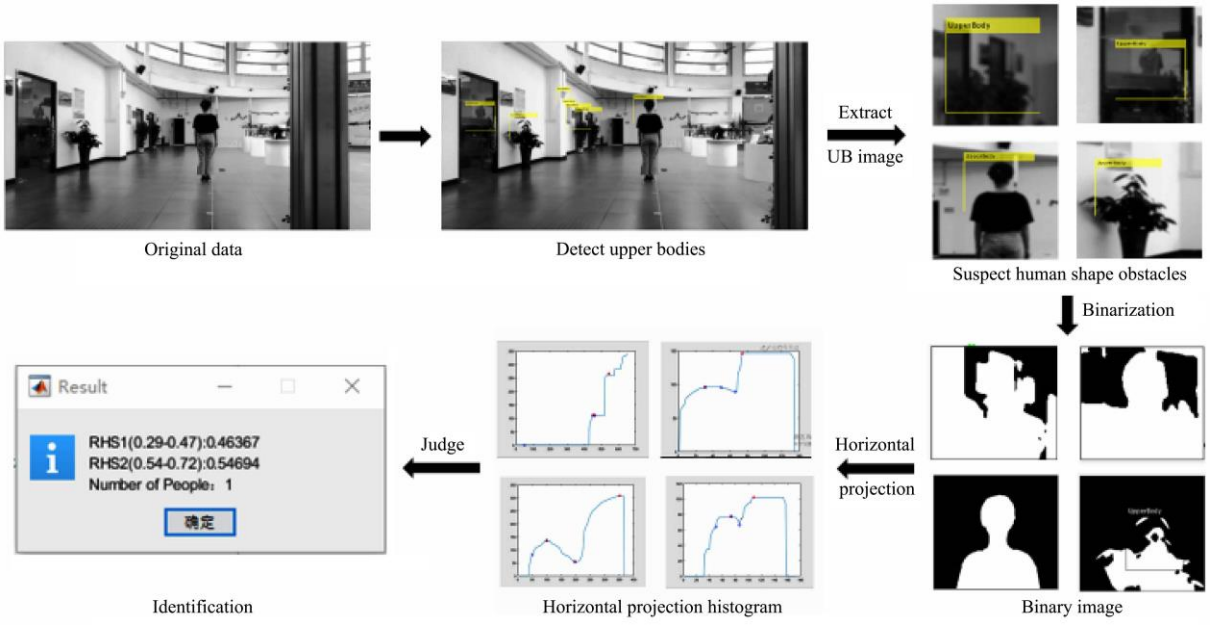

Figure 7 Human-shape obstacles inspection process

Figure 8 Human-shape obstacle on a concrete road in sugar orange orchard

As can be seen from Table 2, within the set test range of 6 meters, the binocular camera has a good depth recognition effect, but in the ratio detection, the R_{HS1} value of 6 m is slightly higher than the judgment range. After inspection, it is found that the upper body of the male tester in the 6-meter picture has a rotation angle. As shown in Figure 9, the position of the mask and ears affects the extraction of the maximum head width W_H.

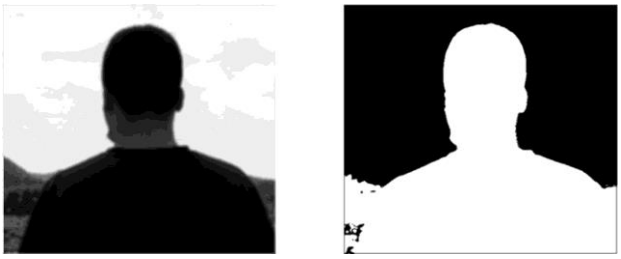

a. Original upper body b. Binary image

Figure 9 Mask and ears affects the extraction of W_H

Because human head and shoulders may have angular deflection, R_{HS1} and R_{HS2} are corrected to ±5% error tolerance range, the error recognition at 6 m is corrected and the recognition rate is also improved. Therefore, judging field humanoid obstacles based on the proportion of the human body on farm roads has good distinguishability. Within the maximum testing range of 6 meters, the relative depth error is within 5%, and the detection time for a human-shape obstacle is less than 150 ms, which meets the obstacle avoidance requirements.

a. Ttest in orchard bush

Original upper body Binary image

b. Uneven illumination

Original upper body Binary image

c. Similar in color

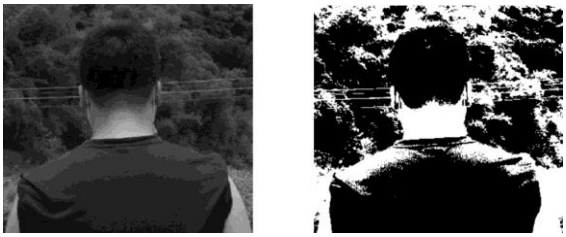

Original upper body Binary image

d. Result of image enhancement processing

Figure 10 human-shape obstacle in the bushes of sugar orange orchard

In the bush test, as shown in Figure 10b, when the illumination is uneven, the original algorithm can extract the upper body and head-shoulder feature points, but the horizontal projection histogram contour is not ideal. When a person's clothing is similar to the background color, as shown in Figure 10c, there will be incomplete outlines or blurred edges in the binary graph, and the head-shoulder feature points of human-shaped obstacles cannot be correctly identified, which causes value of R_{HS1} and R_{HS2} overflows the judgment range. Therefore, homomorphic filtering, image sharpening and other image enhancement processing are added into the algorithm, as shown in Figure 10d, the processed image is with good effect. The head and shoulder feature points can be extracted. Although the arm contour is missing, it does not affect the judgment of head-shoulder proportion.

4 Conclusions

According to the human appearance scene in farmland, head-shoulder ratio characteristics and basic spraying parameters, this paper proposes a field human-shape obstacle recognition method based on Viola-Jones Algorithm, and validates the method in indoor and outdoor environments. The proposed Viola-Jones Algorithm method is capable of identifying human-shaped obstacles on the front or back of the field.

The cascade object detector can be used to obtain the upper body within the view scope of particular angle, but in the **b**inary images, the width of head and shoulders change with ears, hair, accessories, clothes, etc., also affected by environmental factors such as light, the shooting angle. The next research can be combined with Full-body Human Detector, Pedestrian Detection, Face Recognition (including the ear), which will broaden the recognition scene and type, improve the recognition algorithm of farmland humanoid obstacles.

At present, this article only selects the head- shoulder ratio characteristics of Chinese adults and it is only suitable for the rapid and preliminary analysis of human-shape obstacles in China. The detection in complex background and recognition of other farmland obstacles are still difficult problems in the study of obstacle avoidance in farmland.

Funding

This research was funded by the Key Field R&D Program of Guangdong Province, China, grant number 2019B020221001,the 111 Project, grant number D18019, the Science and Technology Planning Project of Guangdong Province, China, grant number 2018A050506073 and the Science and Technology Planning Project of Guangzhou city, China, grant number 201807010039.

Acknowledgments

This research was supported by Supernode Innovative Technology Co., Ltd.

[References]

[1] Wang L L, Lan Y B, Zhang Y L, et al. Applications and prospects of agricultural unmanned aerial vehicle obstacle avoidance technology in China. Sensors, 2019; 19(3): 642. doi: 10.3390/s19030642

[2] Ministry of Industry and Information Technology of the People's Republic of China. Available online: http://www.miit.gov.cn/n1146285/n1146352/n3054355/n7697926/n7697940/c7715291/content.html(accessed on 26 1 2018).

[3] Lan Y B, Wang G B. Development Situation and Prospect of Plant Protection UAV Industry in China. Agricultural Engineering Technology, 2018; 38, 17–27. (in Chinese) doi: 10.16815/j.cnki.11-5436/s.2018.09

[4] Lan Y B, Chen S D. Current status and trends of plant protection UAV and its spraying technology in China. Int J Precis Agric Aviat, 2018; 1(1): 1–9. doi: 10.33440 / j.ijpaa.20180101.0002

[5] Dalal N, Triggs B. Histograms of oriented gradients for human detection. 2005 IEEE computer society conference on computer vision and pattern recognition (CVPR'05). IEEE, 2005, 1: 886-893. doi: 10.1109/CVPR.2005.177

[6] Guo Z, Zhang L, Zhang D. Rotation invariant texture classification using LBP variance (LBPV) with global matching. Pattern recognition, 2010, 43(3): 706–719. doi: 10.1016/j.patcog.2009.08.017

[7] Papageorgiou C P, Oren M, Poggio T. A general framework for object detection. Sixth International Conference on Computer Vision (IEEE Cat. No. 98CH36271). IEEE, 1998: 555-562.doi:10.1109/ICCV.1998.710772

[8] Lienhart R, Maydt J. An extended set of haar-like features for rapid object detection.Proceedings. international conference on image processing. IEEE, 2002, 1: I–I. doi: 10.1109 / ICIP.2002.1038171

[9] Wang X, Han T X, Yan S. An HOG-LBP human detector with partial occlusion handling. 2009 IEEE 12th international conference on computer vision. IEEE, 2009: 32-39. doi: 10.1109/ICCV.2009.5459207

[10] Train a Cascade Object Detector. Available online: https://www.mathworks.com/help/vision/ug/train-a-cascade-object-detector.html.

[11] Viola P, Jones M. Rapid object detection using a boosted cascade of simple features. Proceedings of the 2001 IEEE computer society conference on computer vision and pattern recognition. CVPR 2001. IEEE, 2001, 1: I–I. doi: 10.1109 / CVPR.2001.990517

[12] Yang S H, Zheng Y J, Liu X X. Research status and trends of downwash airflow of spray UAVs in agriculture. Int J Precis Agric Aviat, 2019; 2(1): 1–8. doi: 10.33440 / j.ijpaa.20190201.0023

[13] Kong H, Yi L L, Lan Y B, Kong F X, Han X. Exploring the operation mode of spraying cotton defoliation agent by plant protection UAV. Int J Precis Agric Aviat, 2020; 3(1): 43–48. doi: 10.33440/j.ijpaa.20200301.65

[14] Bux A, Angelov P, Habib Z. Vision based human activity recognition: a review. Advances in Computational Intelligence Systems. Springer, Cham, 2017; 341–371.

[15] Benfold B, Reid I. Stable multi-target tracking in real-time surveillance video. CVPR 2011. IEEE, 2011: 3457–3464. doi: 10.1109 / CVPR.2011.5995667

[16] Ding Y L. Man Machine Engineering (5th edition).Beijing: Beijing Institute of Technology Press (BITP), 2015. (in Chinese)

[17] National Health Commission of the People's Republic of China. Available online: http://www.nhc.gov.cn/jkj/s5879/201506/4505528e65f3460fb88685081ff158a2.shtml (accessed on 30 6 2015).

[18] Hoai M, Zisserman A. Talking heads: Detecting humans and recognizing their interactions. Proceedings of the IEEE Conference on Computer Vision and Pattern Recognition, 2014: 875–882.

[19] Xiao H J, Zhao S G, Zhang L. Head-shoulder detection HOG-LBP based feature fusion. Microcomputer & its applications, 2015, 34(5): 43–46. (in Chinese) doi: 10.3969/j.issn.1674-7720.2015.05.015

[20] vision.CascadeObjectDetector. Available online: https://www.mathworks.com/help/vision/ref/vision.cascadeobjectdetector-system-object.html.

[21] Otsu N. A Threshold Selection Method from Gray-Level Histograms. IEEE Transactions on Systems, Man, and Cybernetics, 1979, 9(1): 62–66. doi: 10.1109/TSMC.1979.4310076

[22] Chen H W, McGurr M. Moving human full body and body parts detection, tracking, and applications on human activity estimation, walking pattern and face recognition. Automatic Target Recognition XXVI. International Society for Optics and Photonics, 2016, 9844: 98440T. doi: 10.1117/12.2224319

[23] Dollár P, Wojek C, Schiele B, et al. Pedestrian detection: A benchmark. 2009 IEEE Conference on Computer Vision and Pattern Recognition. IEEE, 2009: 304-311. doi: 10.1109 / CVPR.2009.5206631